

Quasiparticle Properties of a Mobile Impurity in a Bose-Einstein Condensate

Rasmus Søggaard Christensen,¹ Jesper Levinsen,^{2,3} and Georg M. Bruun¹

¹*Department of Physics and Astronomy, Aarhus University, DK-8000 Aarhus C, Denmark*

²*School of Physics and Astronomy, Monash University, Victoria 3800, Australia*

³*Aarhus Institute of Advanced Studies, Aarhus University, DK-8000 Aarhus C, Denmark*

(Dated: October 1, 2018)

We develop a systematic perturbation theory for the quasiparticle properties of a single impurity immersed in a Bose-Einstein condensate. Analytical results are derived for the impurity energy, the effective mass, and residue to third order in the impurity-boson scattering length. The energy is shown to depend logarithmically on the scattering length to third order, whereas the residue and effective mass are given by analytical power series. When the boson-boson scattering length equals the boson-impurity scattering length, the energy has the same structure as that of a weakly interacting Bose gas, including terms of the Lee-Huang-Yang and fourth order logarithmic form. Our results, which cannot be obtained within the canonical Fröhlich model of an impurity interacting with phonons, provide valuable benchmarks for many-body theories and for experiments.

The problem of an impurity interacting with a reservoir with a continuous set of degrees of freedom plays a fundamental role in our understanding of many-body quantum systems. Landau and Pekar famously demonstrated that electrons in a dielectric medium become dressed by phonons forming a quasiparticle termed a polaron [1, 2]. Other examples of mobile impurities include helium-3 mixed with helium-4 [3] and Λ particles in nuclear matter [4]. Static impurities give rise to the Anderson orthogonality catastrophe [5] and the Kondo effect [6]. With the creation of two-component atomic gases characterized by an unrivaled experimental flexibility, the impurity problem can now be studied more systematically and from a broader perspective. While focus has mostly been on impurities in a Fermi sea (the Fermi polaron) [7–9], there have been some experiments on impurity atoms in a Bose gas [10–15]. With the recent identification of Feshbach resonances in Bose-Fermi [16–18] and Bose-Bose [19, 20] mixtures, the study of impurity physics in a Bose-Einstein condensate (BEC) with a tunable interaction is now within reach.

The impurity problem provides an ideal setting for testing many-body theories, and it has yielded fundamental insights for the Fermi polaron [21]. In the case of an impurity atom in a BEC—the Bose polaron—most studies have either used mean-field theory to study self-localization [22–25] and time dependence for weak coupling [26], or employed an effective Fröhlich model which is solved using various many-body techniques [27–32]. The Fröhlich model, however, ignores interaction terms important even for weak coupling, as we shall demonstrate. The correct microscopic Hamiltonian has been used in a field theoretic approach, selectively summing ladder diagrams [33], and in a variational approach [34].

Since the impurity problem is so useful as a theoretical testing ground, it is important to have a quantitatively reliable theory, which can serve as a benchmark for other many-body theories and for experiments in the weak coupling regime. Here, we provide such an accurate theory

by developing a systematic perturbation expansion for the impurity self-energy to *third order* in the impurity-boson scattering length a . The small parameter of this expansion is a/ξ , with ξ being the BEC coherence length. Also, $a^2/\xi a_B$ has to be small for the polaron to be well defined, where a_B is the boson-boson scattering length. We derive analytical results for the zero temperature quasiparticle properties of the polaron, showing that the energy contains a logarithmic term $\ln(a^*/\xi)a^3/\xi^3$, where $a^* \sim \max(a, a_B)$. When $a = a_B$, the perturbative expression for the energy has the same form as the celebrated result for a weakly interacting Bose gas [35–39]. The quasiparticle residue and the effective mass are, on the other hand, given by analytic power series up to a^3/ξ^3 . We use a \mathcal{T} -matrix approach, a technique which has previously been employed for the Fermi polaron to sum diagrams to high order with Monte Carlo methods [40–42]. Our approach uses the correct microscopic Hamiltonian rather than the Fröhlich model used in Refs. [27–32], as the latter is symmetric with respect to the sign of the interaction and therefore only contains even powers in perturbation theory beyond the mean-field shift. Also, the field theory [33] and the variational approach [34] miss terms at second order.

We consider an impurity of mass m immersed in a BEC of particles with mass m_B . The Hamiltonian is

$$H = \sum_{\mathbf{k}} \epsilon_{\mathbf{k}}^B a_{\mathbf{k}}^\dagger a_{\mathbf{k}} + \frac{1}{2\mathcal{V}} \sum_{\mathbf{k}, \mathbf{k}', \mathbf{q}} V_B(q) a_{\mathbf{k}+\mathbf{q}}^\dagger a_{\mathbf{k}'-\mathbf{q}}^\dagger a_{\mathbf{k}'} a_{\mathbf{k}} + \sum_{\mathbf{k}} \epsilon_{\mathbf{k}} c_{\mathbf{k}}^\dagger c_{\mathbf{k}} + \frac{1}{\mathcal{V}} \sum_{\mathbf{k}, \mathbf{k}', \mathbf{q}} V(q) c_{\mathbf{k}+\mathbf{q}}^\dagger a_{\mathbf{k}'-\mathbf{q}}^\dagger a_{\mathbf{k}'} c_{\mathbf{k}}, \quad (1)$$

where $a_{\mathbf{k}}$ and $c_{\mathbf{k}}$ removes a boson and an impurity, respectively, with momentum \mathbf{k} , $\epsilon_{\mathbf{k}}^B = k^2/2m_B$ and $\epsilon_{\mathbf{k}} = k^2/2m$ are the free dispersions, and \mathcal{V} is the system volume. The boson-boson $V_B(q)$ and boson-impurity interaction $V(q)$ are assumed to be short ranged, and they give the usual zero energy scattering matrices $\mathcal{T}_B = 4\pi a_B/m_B$ and $\mathcal{T}_v = 2\pi a/m_r$ respectively, with $m_r =$

$m_B m / (m_B + m)$ the reduced mass, see the Supplemental Material [43]. We work in units where $\hbar = k_B = 1$.

The BEC is assumed to be weakly interacting such that it can be described by Bogoliubov theory, *i.e.* $n_0 a_B^3 \ll 1$ with n_0 being the condensate density. We define the imaginary time Bose Green's functions as $G_{11}(\mathbf{k}, \tau) = -\langle T_\tau \{a_{\mathbf{k}}(\tau), a_{\mathbf{k}}^\dagger(0)\} \rangle$, $G_{12}(\mathbf{k}, \tau) = -\langle T_\tau \{a_{-\mathbf{k}}(\tau), a_{\mathbf{k}}(0)\} \rangle$ and $G_{21}(\mathbf{k}, \tau) = -\langle T_\tau \{a_{\mathbf{k}}^\dagger(\tau), a_{-\mathbf{k}}^\dagger(0)\} \rangle$, where T_τ denotes time ordering. The Fourier transforms are

$$G_{11}(\mathbf{k}, z) = \frac{u_{\mathbf{k}}^2}{z - E_{\mathbf{k}}} - \frac{v_{\mathbf{k}}^2}{z + E_{\mathbf{k}}}, \quad G_{12}(\mathbf{k}, z) = \frac{u_{\mathbf{k}} v_{\mathbf{k}}}{E_{\mathbf{k}}^2 - z^2},$$

with $u_{\mathbf{k}}^2 = (\xi_{\mathbf{k}}/E_{\mathbf{k}} + 1)/2$, $v_{\mathbf{k}}^2 = (\xi_{\mathbf{k}}/E_{\mathbf{k}} - 1)/2$, $E_{\mathbf{k}} = \sqrt{\xi_{\mathbf{k}}^2 - \mathcal{T}_B^2 n_0^2}$, $\xi_{\mathbf{k}} = \epsilon_{\mathbf{k}}^B + \mathcal{T}_B n_0$, and $G_{21}(\mathbf{k}, z) = G_{12}(\mathbf{k}, z)$. Here, $z = i2sT$ is a Bose Matsubara frequency, s is an integer, and T is the temperature,

Perturbation series.—Our aim is to develop a systematic perturbation theory in powers of the impurity-boson scattering length for the quasiparticle properties of the impurity. To this end, we write down all diagrams for the impurity self-energy up to third order in the bare interaction $V(q)$. We then formally replace $V(q)$ with \mathcal{T}_v in each diagram. Diagrams which contain the simultaneous forward propagation of an impurity and a boson (the pair propagator), such as the second order diagram in Fig. 1(a) and the three first third order diagrams in Fig. 2(a), can be thought of as coming from the expansion

$$\mathcal{T}(p) = \frac{\mathcal{T}_v}{1 - \mathcal{T}_v \Pi_{11}(p)} = \mathcal{T}_v + \mathcal{T}_v^2 \Pi_{11}(p) + \dots \quad (2)$$

of the ladder approximation for the impurity-boson scattering matrix in the BEC [44]. Here, $\Pi_{11}(p)$ denotes the pair propagator regularized by subtracting the vacuum scattering already contained in \mathcal{T}_v . We use the shorthand notation $p = (\mathbf{p}, \omega)$ having analytically continued to real energy $z \rightarrow \omega + i0_+$. The perturbative expansion (2) is convergent only for small $\mathcal{T}_v \Pi_{11}(p)$, *i.e.* small a , whereas the full frequency dependence of $\mathcal{T}(p)$ has to be retained when a is large. This approach, which is detailed in the Supplemental Material, yields a perturbation series in a for the self-energy: $\Sigma(p) = \Sigma_1(p) + \Sigma_2(p) + \Sigma_3(p) + \dots$, where Σ_n contains diagrams of order a^n . The first order term is the mean-field energy shift $\mathcal{T}_v n$ with n being the total boson density. We now evaluate the next two terms.

Second order.—We now evaluate the next two terms. Second order. The six second order self-energy diagrams are shown in Fig. 1. Fig. 1(a) is given by $n_0 \mathcal{T}_v^2 \Pi_{11}$ and—together with Fig. 1(e)—comes from expanding the \mathcal{T} -matrix given by Eq. (2) to second order in a inside the ladder approximation to the self-energy. The three diagrams in Figs. 1(b)–(d) are given by $n_0 \mathcal{T}_v^2 \Pi_{22}$, $n_0 \mathcal{T}_v^2 \Pi_{21}$, and $n_0 \mathcal{T}_v^2 \Pi_{12}$, respectively, with $\Pi_{21} = \Pi_{12}$ representing the anomalous propagators and Π_{22} the particle-hole propagator [43]. Apart from ladder summations inside

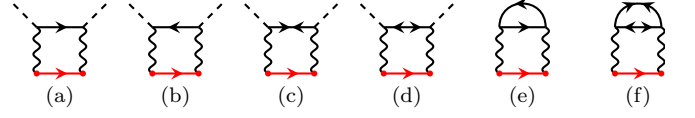


FIG. 1. Second order diagrams for the self-energy. The upper solid black lines are the normal, G_{11} , and anomalous, G_{12} and G_{21} , boson propagators. The dashed lines are particles emitted from or absorbed into the BEC, the bottom red lines are the impurity propagators, and the external impurity propagators are attached to the red dots. The wavy lines denote the impurity-boson vacuum scattering matrix \mathcal{T}_v . All diagrams come from ladder-type diagrams similar to those arising in Eq. 2: The pair propagator Π_{11} appears in (a) and (e), Π_{22} in (b), Π_{12} in (c), and Π_{21} in (d) and (f).

\mathcal{T}_v , the first four diagrams in Fig. 1 only contain scattering of bosons into or out of the BEC, and they can in fact be obtained from the Fröhlich model if one replaces $g \rightarrow \mathcal{T}_v$ by hand [27]. Figures 1(e) and (f) contain vertices where both the in- and outgoing bosons are outside the BEC, and they are not included in the Fröhlich model. They are, however suppressed by a factor $(n_0 a_B^3)^{1/2}$, and since we only consider terms to lowest order in $n_0 a_B^3$, these two diagrams will be ignored. Likewise, we do not distinguish between n_0 and n in the following.

In total, the second order self-energy is

$$\Sigma_2(p) = n_0 \mathcal{T}_v^2 [\Pi_{11}(p) + 2\Pi_{12}(p) + \Pi_{22}(p)]. \quad (3)$$

For $T = 0$ and $p = (\mathbf{0}, 0)$, $\Pi_{11}(p)$, $\Pi_{12}(p)$, and $\Pi_{22}(p)$ may be found analytically [43] to yield

$$\Sigma_2(0) = A(\alpha) \frac{2\pi n_0}{m_r} \frac{a^2}{\xi}, \quad (4)$$

where $\alpha \equiv m/m_B$ is the mass ratio and $\xi = 1/\sqrt{8\pi n a_B}$ is the coherence length of the BEC. We have $A(1) = 8\sqrt{2}/3\pi$, and $A(\alpha)$ for a general mass ratio is given analytically in the Supplemental Material [43].

Third order.—We now consider the diagrams for $\Sigma_3(p)$. They can be divided into three different classes. The first, denoted $\Sigma_{3a}(p)$, is obtained by inserting first order self-energies $\mathcal{T}_v n_0$ for the impurity propagators in the second order diagrams depicted in Figs. 1(a)–(d). This yields four diagrams which are easily evaluated. As we shall see, however, these self-energy insertions are canceled by a similar first order shift $\mathcal{T}_v n_0$ in the impurity energy, which must be inserted in the second order diagrams.

The second class of third order diagrams consists of the eight “ladder” diagrams depicted in Fig. 2(a). They are easily expressed in terms of the two-particle propagators Π_{ij} . Using the effective propagator $G = G_1 = G_2$, with $G_1 = G_{11} + G_{12}$ and $G_2 = G_{11} + G_{21}$, they can be reduced to the two diagrams shown in Fig. 2(b). Their sum is

$$\Sigma_{3b} = n_0 \mathcal{T}_v^3 [(\Pi_{11} + \Pi_{12})^2 + (\Pi_{22} + \Pi_{12})^2], \quad (5)$$

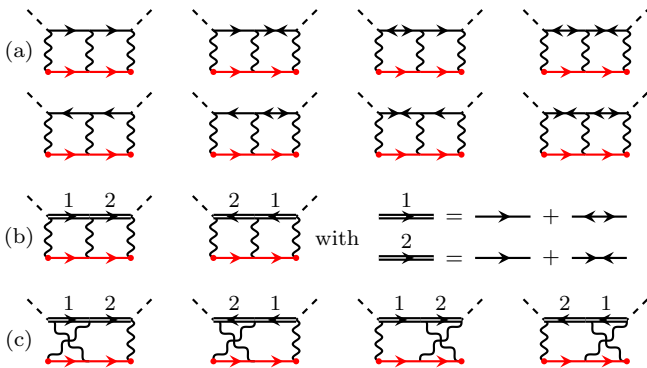


FIG. 2. Third order diagrams for the self-energy: (a) Σ_{3b} , (b) Σ_{3b} expressed using the propagator $G(p)$, and (c) Σ_{3c} .

where we have suppressed the momentum and frequency dependence for notational simplicity.

The third class of diagrams are those where either the first or the last two interaction lines are crossed. There are 16 such diagrams, but using the propagator $G(p)$ they can be reduced to the four terms depicted in Fig. 2(c), which constitutes a major simplification. Evaluating the Matsubara sums and specializing to $T = 0$ yields for the sum of the crossed diagrams

$$\Sigma_{3c}(p) = 2n_0 \mathcal{T}_v^3 \int d\tilde{k} \left\{ \frac{v_{\tilde{k}}^2 - u_{\tilde{k}} v_{\tilde{k}}}{z - E_{\tilde{k}} - \epsilon_{\tilde{k}'}} [\Pi_{11}(k') + \Pi_{12}(k')] + \frac{u_{\tilde{k}}^2 - u_{\tilde{k}} v_{\tilde{k}}}{z - E_{\tilde{k}} - \epsilon_{\tilde{k}'}} [\Pi_{22}(k') + \Pi_{12}(k')] \right\}, \quad (6)$$

with $k' \equiv (\mathbf{p} + \mathbf{k}, z - E_{\mathbf{k}})$.

Equation (6) is, in fact, ultraviolet divergent, the offending terms being $u_{\tilde{k}} v_{\tilde{k}} \Pi_{11}(k')$ and $u_{\tilde{k}}^2 \Pi_{12}(k')$. As shown in the Supplemental Material [43], these two terms give rise to a $1/k$ behavior of the integrand for Σ_{3c} for large k , which thus appears to be logarithmically divergent. However, this should not cause us too much worry. First, the integrand is well behaved at low momenta, where a natural lower cutoff is provided by $k \sim 1/\xi$, below which the boson dispersion becomes linear. Second, the ultraviolet divergence is a consequence of the fact that we have assumed a constant scattering matrix \mathcal{T}_B . Retaining the energy dependence of \mathcal{T}_B would result in an ultraviolet cutoff $\sim 1/a_B$. Likewise, replacing \mathcal{T}_v by the full energy dependent scattering matrix \mathcal{T} in the diagrams for Σ_{3c} gives a cutoff $\sim 1/a$. We can therefore write

$$\Sigma_3(0) = B(\alpha) \frac{2\pi n_0}{m_r} \frac{a^3}{\xi^2} \ln(a^*/\xi) + \mathcal{O}(a^3/\xi^3), \quad (7)$$

with $a^* \equiv \max(a, a_B)$. For the equal mass case we have $B(1) = 2/3 - \sqrt{3}/\pi$, and the analytic expression for general α is given in the Supplemental Material [43]. Note that since $\Sigma_{3b}(p) \sim \mathcal{O}(a^3/\xi^3)$, it does not contribute to the self-energy to the order stated in Eq. (7) for $a > a_B$.

It does, however, contribute to the quasiparticle residue and effective mass, as we shall see below.

Quasiparticle energy.—Having evaluated the 28 third order diagrams, we can now present a perturbative expression for the polaron energy given by the solution of $E(\mathbf{p}) = \mathbf{p}^2/2m + \Sigma[\mathbf{p}, E(\mathbf{p})]$. From Eqs. (4) and (7), we obtain for $\mathbf{p} = \mathbf{0}$ and $T = 0$

$$\frac{E(0)}{\Omega} = \frac{a}{\xi} + A(\alpha) \frac{a^2}{\xi^2} + B(\alpha) \frac{a^3}{\xi^3} \ln(a^*/\xi) \quad (8)$$

where $\Omega = 2\pi n_0 \xi/m_r$ is the mean-field polaron energy for $a = \xi$. Equation (8) gives the polaron energy to order $\ln(a^*/\xi) a^3/\xi^3$ and is one of our main results. We see that the small parameter of the perturbation series is a/ξ . The second order term agrees with that obtained using the Fröhlich Hamiltonian [29]. As we can see from Fig. 2(b) however, the third order logarithmic term comes from scattering events where both bosons are excited out of the BEC. These are precisely the processes ignored by the Fröhlich model, which therefore incorrectly predicts a vanishing third order term. On the other hand, at fourth order in a the Fröhlich model has been shown to also have a logarithmic contribution [31].

Interestingly, when $a = a_B$, Eq. (8) has the same structure as the famous result for the energy of a weakly interacting Bose gas: schematically $E \sim a[1 + (na^3)^{3/2} + na^3 \ln(na^3)]$ [44]. Since it is difficult to measure the bulk energy of a Bose gas, the Lee-Huang-Yang $(na^3)^{3/2}$ term [35, 36] was measured only recently [45], whereas the logarithmic correction [37–39] has never been detected. The energy of an impurity atom has, however, been measured accurately using radio-frequency (rf) spectroscopy [7–9], and our result therefore suggests a way to measure beyond mean-field effects in Bose gases including logarithmic corrections for the first time.

Quasiparticle residue and effective mass.—The quasiparticle residue is given by $Z^{-1} = 1 - \partial_\omega \Sigma$. For zero momentum, we obtain to third order

$$1 - Z^{-1} = \partial_\omega \Sigma_2(\mathbf{0}, \omega)|_{\mathcal{T}_v n_0} + \partial_\omega \Sigma_3(\mathbf{0}, \omega)|_0 \\ = \partial_\omega \Sigma_2(\mathbf{0}, \omega)|_0 + \partial_\omega [\Sigma_{3b}(\mathbf{0}, \omega) + \Sigma_{3c}(\mathbf{0}, \omega)]|_0. \quad (9)$$

The second line follows from inserting the first order shift $\omega = \mathcal{T}_v n_0$ into the second order self-energy. When expanding in $\mathcal{T}_v n_0$, this yields a third order term, which cancels the third order diagrams Σ_{3a} ; see the Supplemental Material [43]. Contrary to the case of the energy, the self-energy term Σ_{3b} contributes to the residue since $\partial_\omega \Sigma_{3b}$ and $\partial_\omega \Sigma_{3c}$ are of the same order. We can evaluate $\partial_\omega \Sigma_2$ and $\partial_\omega \Sigma_{3b}$ analytically, whereas $\partial_\omega \Sigma_{3c}$ has to be calculated numerically. We obtain

$$Z^{-1} = 1 + C(\alpha) \frac{a^2}{a_B \xi} + D(\alpha) \frac{a^3}{a_B \xi^2}, \quad (10)$$

where $C(\alpha)$ and $D(\alpha)$ are given in the Supplemental Material [43]. For $m = m_B$, we have $C(1) = 2\sqrt{2}/3\pi$ and

$D(1) \approx 0.64$. Equation (10) explicitly shows that the polaron is well defined only for $a^2/a_B\xi \ll 1$.

For an ideal BEC with $a_B = 0$, we have $\xi \rightarrow \infty$, and it follows from Eq. (8) that there are no corrections to the mean-field energy up to third order in a . However, in this limit Eq. (10) predicts $Z = 0$ so that there is no well-defined quasiparticle, signaling a breakdown of perturbation theory. The reason is that the energy of the impurity atom is right at the threshold of the particle-hole continuum of the BEC, giving rise to a square root energy dependence of the self-energy and thus zero residue as explained in the Supplemental Material [43]. Equivalently, Landau's critical velocity $c = (4\pi a_B n)^{1/2}/m_B$ above which the polaron decays through momentum relaxation, is zero for a noninteracting BEC.

The effective mass of the quasiparticle is obtained from $m/m^* = Z(1 + 2m\partial_{p^2}\Sigma)$. Following steps analogous to the calculation of Z , we obtain

$$\frac{m^*}{m} = 1 + F(\alpha)\frac{a^2}{a_B\xi} + G(\alpha)\frac{a^3}{a_B\xi^2}, \quad (11)$$

where $F(\alpha)$ and $G(\alpha)$ are given in the Supplemental Material [43]. For the equal mass case, we have $F(1) = 16\sqrt{2}/45\pi$ and $G(1) \approx 0.37$. Our result for $F(\alpha)$ matches that of Ref. [29].

Plots.—In Fig. 3, we plot the zero momentum polaron energy, residue, and effective mass, obtained from Eqs. (8), (10), and (11), in the range $-0.3 < a/\xi < 0.3$ where we expect perturbation theory to be reliable. As was discussed above, one should be careful when a_B approaches zero since the quasiparticle residue vanishes in this limit. We have chosen $a_B/\xi = 0.1$ and depict the results in the case of equal masses ($\alpha = 1$), as well as for the mass ratios $\alpha = 39/87$ and $\alpha = 87/39$ corresponding to the experimentally relevant case of a ^{39}K - ^{87}Rb mixture.

Consider first the energy. We have $E(0) < 0$ [$E(0) > 0$] for $a < 0$ [$a > 0$], corresponding to the attractive (repulsive) branch which are both described within our perturbation theory. The second order term gives a significant correction to the energy whereas the third order term is very small. This is explained in the inset, which shows that the third order expansion coefficient $B(\alpha)$ is much smaller than the second order coefficient $A(\alpha)$, except for $\alpha \ll 1$, so that the third order term is suppressed even when $a/\xi \sim 1$. In fact, $B(\alpha) \rightarrow 0$ for a very heavy impurity with $\alpha \rightarrow \infty$ [43]. We note that the polaron can form a dimer with a boson for $a > 0$. This decay process is, however, slow in the perturbative regime considered here, since the molecule is deeply bound with a binding energy $-1/2m_r a^2$.

Consider next the quasiparticle residue Z . Here, the third order term gives a significant correction, increasing Z for the attractive polaron and decreasing it for the repulsive polaron. As we see from the inset, this is because the third order coefficient $D(\alpha)$ is larger than the second order coefficient $C(\alpha)$. Finally, we see that

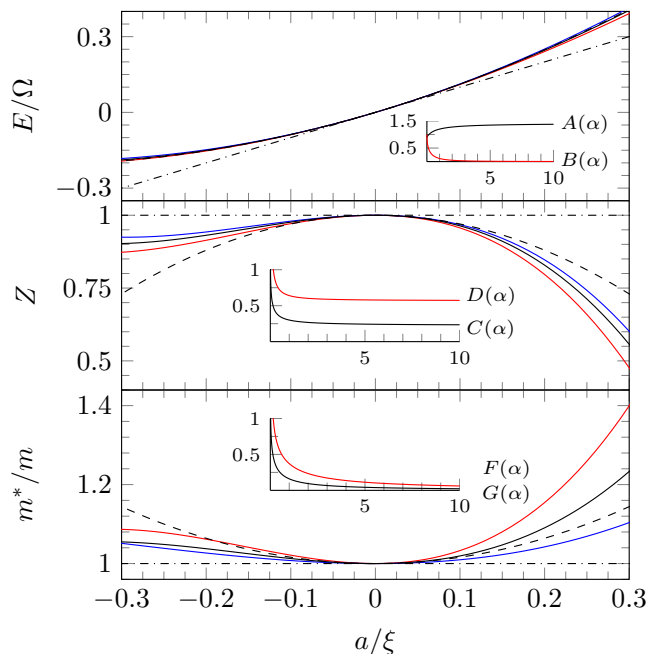


FIG. 3. The polaron energy E , residue Z and effective mass m^* as given by Eqs. (8), (10), and (11) for $a_B/\xi = 0.1$. We show the first order term (dash-dotted lines), second order (dashed lines) and third order (solid lines) for equal masses (black lines). For $\alpha = 39/87$ (red lines) and $\alpha = 87/39$ (blue lines) we only show the third order result. In the insets, we show the relevant second and third order expansion coefficients as a function of mass ratio.

the third order term gives a large contribution to the effective mass, decreasing (increasing) it for the attractive (repulsive) polaron. This is consistent with the inset depicting the expansion coefficients $F(\alpha)$ and $G(\alpha)$. We have $F(\alpha) \rightarrow 0$ and $G(\alpha) \rightarrow 0$ for $\alpha \rightarrow \infty$ [43], indicating that the effective mass equals the bare mass for a very heavy impurity as expected.

Varying ξ/a_B changes the slope of m^* and Z as a function of a/ξ , but the results are qualitatively the same as those depicted in Fig. 3. Varying the mass ratio α also changes the relative weight of the second and third order terms as explained above. In the Supplemental Material, we provide the values of $A(\alpha), \dots, G(\alpha)$ for $\alpha = 0$ and $\alpha \rightarrow \infty$. Intriguingly, $C(\alpha)$, $D(\alpha)$, $F(\alpha)$, and $G(\alpha)$ all diverge for $\alpha \rightarrow 0$, indicating a breakdown of perturbation theory. In this limit, the atoms in the BEC are much heavier than the impurity, and it would be interesting to examine how this breakdown is related to the problem of a mobile impurity interacting with static scatterers.

Conclusion.—We developed a systematic perturbation theory for the quasiparticle properties of an impurity particle in a BEC. Analytical results for the energy, residue, and effective mass were derived, and the energy was shown to contain a third order logarithmic term, whereas the residue and the effective mass are given by analytic

power series in a up to third order. When $a_B = a$, we obtained the same form for the energy as that of a weakly interacting Bose gas, which opens up the possibility of detecting corrections to mean-field theory of the Lee-Huang-Yang and even a fourth order logarithmic type for the first time, using rf spectroscopy. The effects of a mass difference between the impurity and the atoms in the BEC were analyzed throughout. By deriving rigorous results for the quasiparticle properties of the Bose polaron, our theory provides a useful benchmark for approximate many-body theories and for experiments.

We thank M. M. Parish, R. Schmidt, Y. Nishida, and J. Arlt for useful discussions. R.S.C. and G.M.B. would like to acknowledge the support of the Villum Foundation via Grant No. VKR023163.

-
- [1] L. D. Landau, Phys. Z. Sowjetunion **3**, 644 (1933).
 [2] S. I. Pekar, Zh. Eksp. Teor. Fiz. **16**, 335 (1946).
 [3] G. Baym and C. Pethick, *Landau Fermi-Liquid Theory: Concepts and Applications* (Wiley-VCH, 1991).
 [4] R. Bishop, Annals of Physics **78**, 391 (1973).
 [5] P. W. Anderson, Phys. Rev. Lett. **18**, 1049 (1967).
 [6] J. Kondo, Prog. Theor. Phys. **32**, 37 (1964).
 [7] A. Schirotzek, C.-H. Wu, A. Sommer, and M. W. Zwierlein, Phys. Rev. Lett. **102**, 230402 (2009).
 [8] C. Kohstall, M. Zaccanti, M. Jag, A. Trenkwalder, P. Massignan, G. M. Bruun, F. Schreck, and R. Grimm, Nature (London) **485**, 615 (2012).
 [9] M. Koschorreck, D. Pertot, E. Vogt, B. Fröhlich, M. Feld, and M. Köhl, Nature (London) **485**, 619 (2012).
 [10] J. Catani, G. Lamporesi, D. Naik, M. Gring, M. Inguscio, F. Minardi, A. Kantian, and T. Giamarchi, Phys. Rev. A **85**, 023623 (2012).
 [11] T. Fukuhara, A. Kantian, M. Endres, M. Cheneau, P. Schausz, S. Hild, D. Bellem, U. Schollwöck, T. Giamarchi, C. Gross, I. Bloch, and S. Kuhr, Nature Physics **9**, 235 (2013).
 [12] S. Palzer, C. Zipkes, C. Sias, and M. Köhl, Phys. Rev. Lett. **103**, 150601 (2009).
 [13] A. P. Chikkatur, A. Görlitz, D. M. Stamper-Kurn, S. Inouye, S. Gupta, and W. Ketterle, Phys. Rev. Lett. **85**, 483 (2000).
 [14] N. Spethmann, F. Kindermann, S. John, C. Weber, D. Meschede, and A. Widera, Phys. Rev. Lett. **109**, 235301 (2012).
 [15] R. Scelle, T. Rentrop, A. Trautmann, T. Schuster, and M. K. Oberthaler, Phys. Rev. Lett. **111**, 070401 (2013).
 [16] C.-H. Wu, J. W. Park, P. Ahmadi, S. Will, and M. W. Zwierlein, Phys. Rev. Lett. **109**, 085301 (2012).
 [17] M.-S. Heo, T. T. Wang, C. A. Christensen, T. M. Rvachov, D. A. Cotta, J.-H. Choi, Y.-R. Lee, and W. Ketterle, Phys. Rev. A **86**, 021602 (2012).
 [18] T. D. Cumby, R. A. Shewmon, M.-G. Hu, J. D. Perreault, and D. S. Jin, Phys. Rev. A **87**, 012703 (2013).
 [19] G. Roati, M. Zaccanti, C. D’Errico, J. Catani, M. Modugno, A. Simoni, M. Inguscio, and G. Modugno, Phys. Rev. Lett. **99**, 010403 (2007).
 [20] K. Pilch, A. D. Lange, A. Prantner, G. Kerner, F. Ferlaino, H.-C. Nägerl, and R. Grimm, Phys. Rev. A **79**, 042718 (2009).
 [21] P. Massignan, M. Zaccanti, and G. M. Bruun, Reports on Progress in Physics **77**, 034401 (2014).
 [22] G. E. Astrakharchik and L. P. Pitaevskii, Phys. Rev. A **70**, 013608 (2004).
 [23] F. M. Cucchietti and E. Timmermans, Phys. Rev. Lett. **96**, 210401 (2006).
 [24] R. M. Kalas and D. Blume, Phys. Rev. A **73**, 043608 (2006).
 [25] M. Bruderer, W. Bao, and D. Jaksch, EPL (Europhysics Letters) **82**, 30004 (2008).
 [26] A. G. Volosniev, H.-W. Hammer, and N. T. Zinner, ArXiv e-prints (2015), arXiv:1502.05300 [cond-mat.quant-gas].
 [27] B.-B. Huang and S.-L. Wan, Chinese Physics Letters **26**, 080302 (2009).
 [28] J. Tempere, W. Casteels, M. K. Oberthaler, S. Knoop, E. Timmermans, and J. T. Devreese, Phys. Rev. B **80**, 184504 (2009).
 [29] W. Casteels and M. Wouters, Phys. Rev. A **90**, 043602 (2014).
 [30] A. Shashi, F. Grusdt, D. A. Abanin, and E. Demler, Phys. Rev. A **89**, 053617 (2014).
 [31] F. Grusdt, Y. E. Shchadilova, A. N. Rubtsov, and E. Demler, ArXiv e-prints (2014), arXiv:1410.2203 [cond-mat.quant-gas].
 [32] J. Vlietinck, W. Casteels, K. Van Houcke, J. Tempere, J. Ryckebusch, and J. T. Devreese, ArXiv e-prints (2014), arXiv:1406.6506 [cond-mat.quant-gas].
 [33] S. P. Rath and R. Schmidt, Phys. Rev. A **88**, 053632 (2013).
 [34] W. Li and S. Das Sarma, Phys. Rev. A **90**, 013618 (2014).
 [35] T. D. Lee and C. N. Yang, Phys. Rev. **105**, 1119 (1957).
 [36] T. D. Lee, K. Huang, and C. N. Yang, Phys. Rev. **106**, 1135 (1957).
 [37] T. T. Wu, Phys. Rev. **115**, 1390 (1959).
 [38] N. M. Hugenholtz and D. Pines, Phys. Rev. **116**, 489 (1959).
 [39] K. Sawada, Phys. Rev. **116**, 1344 (1959).
 [40] N. Prokof’ev and B. Svistunov, Phys. Rev. B **77**, 020408 (2008).
 [41] N. V. Prokof’ev and B. V. Svistunov, Phys. Rev. B **77**, 125101 (2008).
 [42] J. Vlietinck, J. Ryckebusch, and K. Van Houcke, Phys. Rev. B **87**, 115133 (2013).
 [43] See Supplemental Material.
 [44] A. L. Fetter and J. D. Walecka, *Quantum Theory of Many-Particle Systems* (McGraw-Hill, 1971).
 [45] N. Navon, S. Nascimbène, F. Chevy, and C. Salomon, Science **328**, 729 (2010).
-

Supplemental Materials: Quasiparticle Properties of a Mobile Impurity in a Bose-Einstein Condensate

RENORMALIZATION OF THE CONTACT INTERACTION

We relate the boson-impurity scattering length to the short-range potential $V(p)$ as follows. The Lippmann-Schwinger equation yields the vacuum scattering matrix at vanishing energy in the center-of-mass frame

$$\mathcal{T}_v = \frac{1}{V(0)^{-1} - \Pi_v}, \quad (\text{S1})$$

in terms of the Fourier transform of the potential at zero momentum and the vacuum pair propagator $\Pi_v \equiv \int d\check{k} \frac{1}{k^2/2m_r}$. Here we have defined $d\check{k} \equiv d^3k/(2\pi)^3$. At the same time, the vacuum scattering matrix is related to the boson-impurity scattering length via

$$\mathcal{T}_v = \frac{2\pi a}{m_r}. \quad (\text{S2})$$

Similarly for the boson-boson interaction we have

$$\frac{4\pi a_B}{m_B} = \frac{1}{V_B(0)^{-1} - \Pi_B}, \quad (\text{S3})$$

with $\Pi_B \equiv \int d\check{k} \frac{1}{k^2/m_B}$.

PERTURBATION THEORY IN THE SCATTERING LENGTH AND THE PAIR PROPAGATOR

As explained in the manuscript, to obtain a perturbation theory in the scattering length a , we first write down the diagrams in increasing order of the bare interaction $V(q)$. We then formally replace $V(q)$ with \mathcal{T}_v everywhere, which in addition to the obvious substitution $V(q) \rightarrow \mathcal{T}_v$ in the expressions for the diagrams, has one more effect: In diagrams where the ‘‘bare’’ forward pair propagator appears when expanding in $V(q)$, we use the regularised pair propagator Π_{11} instead when expanding in \mathcal{T}_v . That is, when making the replacement $V(q) \rightarrow \mathcal{T}_v$, we also make the replacement

$$-\frac{1}{\beta} \sum_{\omega_\nu} \int d\check{k} G_{11}(-\mathbf{k}, -i\omega_\nu) G(\mathbf{k} + \mathbf{p}, i\omega_\nu + z) = \int d\check{k} \left[\frac{u_{\mathbf{k}}^2(1 + f_{\mathbf{k}})}{z - E_{\mathbf{k}} - \epsilon_{\mathbf{k}+\mathbf{p}}} + \frac{v_{\mathbf{k}}^2 f_{\mathbf{k}}}{z + E_{\mathbf{k}} - \epsilon_{\mathbf{k}+\mathbf{p}}} \right] \rightarrow$$

$$\Pi_{11}(p) = \int d\check{k} \left[\frac{u_{\mathbf{k}}^2(1 + f_{\mathbf{k}})}{z - E_{\mathbf{k}} - \epsilon_{\mathbf{k}+\mathbf{p}}} + \frac{v_{\mathbf{k}}^2 f_{\mathbf{k}}}{z + E_{\mathbf{k}} - \epsilon_{\mathbf{k}+\mathbf{p}}} + \frac{2m_r}{k^2} \right]. \quad (\text{S4})$$

Here $G(\mathbf{k}, z) = 1/(z - \epsilon_{\mathbf{k}})$ is the non-interacting impurity Green’s function, $i\omega_\nu = i(2\nu + 1)T$ is a Fermi Matsubara frequency, $p = (\mathbf{p}, z)$, $f_{\mathbf{k}} = [\exp(E_{\mathbf{k}}/T) - 1]^{-1}$ is the boson distribution function. The term $2m_r/k^2$ in Eq. (S4) subtracts the contribution already contained within the vacuum scattering, and acts to regularize the pair propagator. It comes from inserting the Lippmann-Schwinger equation (S1) in the ladder approximation for $\mathcal{T}(p)$ [S44].

For $T = 0$ and $p = (0, 0)$, Eq. (S4) can be calculated analytically yielding

$$\Pi_{11}(0) = \frac{m_B}{\sqrt{2\pi^2\xi}} \frac{\alpha}{1 + \alpha} \left[1 - \frac{1 - \alpha}{1 + \alpha} f(\alpha) \right]. \quad (\text{S5})$$

This gives $\Pi_{11}(0) = m_B/2\sqrt{2\pi^2\xi}$ for $\alpha = 1$.

Anomalous and particle-hole propagators

The anomalous and particle-hole propagators are

$$\Pi_{12}(p) = -\frac{1}{\beta} \sum_{\omega_\nu} G_{12}(-\mathbf{k}, -i\omega_\nu) G(\mathbf{k}', i\omega_\nu + z) = \int d\check{k} \left[\frac{u_{\mathbf{k}} v_{\mathbf{k}} (1 + f_{\mathbf{k}})}{E_{\mathbf{k}} + \epsilon_{\mathbf{k}'} - z} + \frac{u_{\mathbf{k}} v_{\mathbf{k}} f_{\mathbf{k}}}{\epsilon_{\mathbf{k}'} - E_{\mathbf{k}} - z} \right], \quad (\text{S6})$$

$$\Pi_{22}(p) = -\frac{1}{\beta} \sum_{\omega_\nu} G_{22}(-\mathbf{k}, -i\omega_\nu) G(\mathbf{k}', i\omega_\nu + z) = \int d\check{k} \left[\frac{u_{\mathbf{k}}^2 f_{\mathbf{k}}}{z + E_{\mathbf{k}} - \epsilon_{\mathbf{k}'}} + \frac{v_{\mathbf{k}}^2 (1 + f_{\mathbf{k}})}{z - E_{\mathbf{k}} - \epsilon_{\mathbf{k}'}} \right], \quad (\text{S7})$$

where $\mathbf{k}' = \mathbf{k} + \mathbf{p}$, and $\Pi_{21}(p) = \Pi_{12}(p)$. For $T = 0$ and $p = (0, 0)$ we obtain

$$\begin{aligned} \Pi_{12}(0) &= \frac{m_{\text{B}}}{\sqrt{2}\pi^2\xi} \frac{\alpha}{1 + \alpha} f(\alpha), \\ \Pi_{22}(0) &= \frac{m_{\text{B}}}{\sqrt{2}\pi^2\xi} \frac{\alpha}{1 - \alpha} [1 - f(\alpha)]. \end{aligned} \quad (\text{S8})$$

These expressions are well defined in the equal mass limit $\alpha \rightarrow 1$, where we have $\Pi_{12}(0) = m_{\text{B}}/2\sqrt{2}\pi^2\xi$ and $\Pi_{22}(0) = -m_{\text{B}}/6\sqrt{2}\pi^2\xi$.

With Eqs. (S5) and (S8), we have analytical expressions for all pair propagators for $p = 0$, which is what we need to obtain analytical results for the polaron self-energy at zero momentum.

LOGARITHMIC DIVERGENCE OF Σ_{3c} AND $B(\alpha)$

Analysing the divergence of Σ_{3c} , we investigate the integrand in eq. (6) in the main manuscript for $k \rightarrow \infty$. We have $u_{\mathbf{k}} \rightarrow 1$, $v_{\mathbf{k}} \rightarrow \mathcal{T}_{\text{B}} n_0 m_{\text{B}}/k^2$, $E_{\mathbf{k}} \rightarrow k^2/2m_{\text{B}}$, and $\Pi_{11}(\mathbf{k}, -E_{\mathbf{k}}) \rightarrow m_r^{3/2} \sqrt{k^2/2m_{\text{B}} + k^2/2M}/\sqrt{2}\pi$ for $k \rightarrow \infty$, where $M = m + m_{\text{B}}$. This gives for $p = (\mathbf{0}, 0)$

$$\lim_{k \rightarrow \infty} \frac{u_{\mathbf{k}} v_{\mathbf{k}} \Pi_{11}(\mathbf{k}, -E_{\mathbf{k}})}{E_{\mathbf{k}} + \epsilon_{\mathbf{k}}} = \frac{\mathcal{T}_{\text{B}} n_0 m_{\text{B}} m_r^2 \sqrt{\alpha^2 + 2\alpha}}{\pi(1 + \alpha)k^3}, \quad (\text{S9})$$

and

$$\lim_{k \rightarrow \infty} \frac{u_{\mathbf{k}}^2 \Pi_{12}(\mathbf{k}, -E_{\mathbf{k}})}{E_{\mathbf{k}} + \epsilon_{\mathbf{k}}} = \frac{\mathcal{T}_{\text{B}} n_0 M m_r^2 (\pi - 2 \arctan \sqrt{\alpha^2 + 2\alpha})}{2\pi k^3}, \quad (\text{S10})$$

where we have used

$$I(\alpha) = \int_0^\infty dx \frac{1}{x} \ln \left[\frac{1 + x^2 + (1 + x)^2/\alpha}{1 + x^2 + (1 - x)^2/\alpha} \right] = \pi^2 - 2\pi \arctan \sqrt{\alpha^2 + 2\alpha}. \quad (\text{S11})$$

Using these limits in eq. (6), we see that the integrand goes as $1/k$ for $k \rightarrow \infty$. Setting the lower and upper limits of the remaining k -integral to $1/\xi$ and $1/a^*$ respectively, we obtain eqs. (7) and (S13).

COEFFICIENTS FOR THE ENERGY: $A(\alpha)$ AND $B(\alpha)$

We find

$$A(\alpha) = \frac{2\sqrt{2}}{\pi} \frac{1}{1 - \alpha} \left[1 - \frac{2\alpha^2}{1 + \alpha} f(\alpha) \right], \quad (\text{S12})$$

with $f(\alpha) \equiv \sqrt{(\alpha + 1)/(\alpha - 1)} \arctan \sqrt{(\alpha - 1)/(\alpha + 1)}$ with the definition $\sqrt{-1} = i$. Note that this expression is well defined in the limit $\alpha \rightarrow 1$ corresponding to equal masses, where we have $A(1) = 8\sqrt{2}/3\pi$.

For the logarithmic term, we find

$$B(\alpha) = (1 + \alpha) \left[1 - \frac{2}{\pi} \arctan \sqrt{\alpha^2 + 2\alpha} \right] - \frac{2\sqrt{\alpha^2 + 2\alpha}}{\pi(1 + \alpha)}. \quad (\text{S13})$$

In the case of equal masses, we have $B(1) = 2/3 - \sqrt{3}/\pi$.

COEFFICIENTS FOR THE RESIDUE: $C(\alpha)$ AND $D(\alpha)$

The contributions to the residue from the second order diagrams $\partial_\omega \Sigma_2(\mathbf{0}, \omega)|_0$ and the third order ‘‘ladder’’ diagrams $\partial_\omega \Sigma_{3b}(\mathbf{0}, \omega)|_0$ can be calculated analytically, while the contribution from the ‘‘crossed’’ diagrams has to be evaluated numerically. We obtain

$$\partial_\omega \Sigma_2(\mathbf{0}, \omega)|_0 = -\frac{1}{\sqrt{2\pi}} \frac{a^2}{a_B \xi} \frac{\alpha+1}{\alpha-1} \left[1 - \frac{2}{\alpha+1} f(\alpha) \right], \quad (\text{S14})$$

$$\partial_\omega \Sigma_{3b}(\mathbf{0}, \omega)|_0 = \frac{1}{\pi^2} \frac{a^3}{a_B \xi^2} \frac{\alpha+1}{\alpha} \left\{ \left(\frac{\alpha+1}{\alpha-1} \right)^2 \left[1 - \frac{2\alpha}{\alpha+1} f(\alpha) \right]^2 - \left[1 + \frac{2\alpha}{\alpha+1} f(\alpha) \right]^2 \right\}, \quad (\text{S15})$$

$$\partial_\omega \Sigma_{3c}(\mathbf{0}, \omega)|_0 = \frac{1}{2\pi^2} \frac{a^3}{a_B \xi^2} \left(\frac{\alpha+1}{\alpha} \right)^3 I_\omega(\alpha) \quad (\text{S16})$$

with

$$\begin{aligned} I_\omega(\alpha) = \int_0^\infty dk \left\{ \frac{k^2 E_k^{(-)}}{[E_k + k^2/\alpha]^2} \int_0^\infty dq \int_{-1}^1 dt \left[\frac{q^2 E_q^{(+)}}{E_k + E_q + (k^2 + q^2 - 2kqt)/\alpha} - \frac{2\alpha}{1+\alpha} \right] \right. \\ + \frac{k^2 E_k^{(-)}}{E_k + k^2/\alpha} \int_0^\infty dq \int_{-1}^1 dt \frac{q^2 E_q^{(+)}}{[E_k + E_q + (k^2 + q^2 - 2kqt)/\alpha]^2} \\ + \frac{k^2 E_k^{(+)}}{[E_k + k^2/\alpha]^2} \int_0^\infty dq \int_{-1}^1 dt \frac{q^2 E_q^{(-)}}{E_k + E_q + (k^2 + q^2 - 2kqt)/\alpha} \\ \left. + \frac{k^2 E_k^{(+)}}{E_k + k^2/\alpha} \int_0^\infty dq \int_{-1}^1 dt \frac{q^2 E_q^{(-)}}{[E_k + E_q + (k^2 + q^2 - 2kqt)/\alpha]^2} \right\} \end{aligned} \quad (\text{S17})$$

a dimensionless integral, and

$$E_p = \sqrt{p^2(p^2 + 1)}, \quad E_p^{(\pm)} = \frac{p^2 \pm E_p}{E_p}. \quad (\text{S18})$$

Thus, the coefficients for the residue given by $Z^{-1} = 1 + C(\alpha)a^2/a_B \xi + D(\alpha)a^3/a_B \xi^2$ are

$$\begin{aligned} C(\alpha) &= \frac{1}{\sqrt{2\pi}} \frac{\alpha+1}{\alpha-1} \left[1 - \frac{2}{\alpha} f(\alpha) \right], \\ D(\alpha) &= -\frac{1}{\pi^2} \frac{a^3}{a_B \xi^2} \frac{\alpha+1}{\alpha} \left\{ \left(\frac{\alpha+1}{\alpha-1} \right)^2 \left[1 - \frac{2\alpha}{\alpha+1} f(\alpha) \right]^2 - \left[1 + \frac{2\alpha}{\alpha+1} f(\alpha) \right]^2 \right\} - \frac{1}{2\pi^2} \left(\frac{\alpha+1}{\alpha} \right)^3 I_\omega(\alpha). \end{aligned} \quad (\text{S19})$$

COEFFICIENTS FOR THE EFFECTIVE MASS: $F(\alpha)$ AND $G(\alpha)$

As for the residue, we can calculate the contributions to the effective mass from the second order diagrams $\partial_{p^2} \Sigma_2(\mathbf{p}, 0)|_0$ and the third order ‘‘ladder’’ diagrams $\partial_{p^2} \Sigma_{3b}(\mathbf{p}, 0)|_0$ analytically, while the contribution from the ‘‘crossed’’ diagrams has to be evaluated numerically. We have

$$2m \partial_{p^2} \Sigma_2(\mathbf{p}, 0)|_0 = \frac{1}{\sqrt{2\pi}} \frac{a^2}{a_B \xi} \frac{1}{(\alpha-1)^2} \left[1 + \alpha^2 - \frac{2}{3} \frac{5\alpha^2 + 1}{\alpha+1} f(\alpha) \right], \quad (\text{S20})$$

$$\begin{aligned} 2m \partial_\omega \Sigma_{3b}(\mathbf{0}, \omega)|_0 &= \frac{1}{3\pi^2} \frac{a^3}{a_B \xi^2} \frac{1}{\alpha-1} \\ &\times \left[\left\{ \frac{3\alpha^2 - 4\alpha - 1}{\alpha} + \frac{2(3\alpha^2 - 2\alpha + 1)}{\alpha+1} f(\alpha) \right\} \left\{ 1 + \frac{2\alpha}{\alpha+1} f(\alpha) \right\} \right. \\ &\quad \left. - \left(\frac{\alpha+1}{\alpha-1} \right)^2 \left\{ \frac{3\alpha^2 + 4\alpha - 1}{\alpha} + \frac{2(3\alpha^2 + 2\alpha + 1)}{\alpha+1} f(\alpha) \right\} \left\{ 1 - \frac{2\alpha}{\alpha+1} f(\alpha) \right\} \right], \end{aligned} \quad (\text{S21})$$

$$2m \partial_\omega \Sigma_{3c}(\mathbf{0}, \omega)|_0 = \frac{1}{6\pi^2} \frac{a^3}{a_B \xi^2} \left(\frac{\alpha+1}{\alpha} \right)^3 I_{p^2}(\alpha) \quad (\text{S22})$$

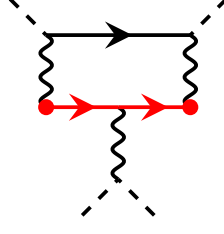


FIG. S1. Third order diagram for the self-energy obtained by a self-energy insertion in the second order ladder diagram.

with

$$\begin{aligned}
I_{p^2}(\alpha) = \int_0^\infty dk \left\{ \frac{4k^3}{\alpha[E_k + k^2/\alpha]^2} \int_0^\infty dq q^2 \int_{-1}^1 dt \frac{k - qt}{[E_k + E_q + (k^2 - 2kqt + q^2)/\alpha]^2} \left(E_k^{(-)} E_q^{(+)} + E_k^{(+)} E_q^{(-)} \right) \right. \\
- \frac{k^2[3E_k - k^2/\alpha]}{[E_k + k^2/\alpha]^3} \int_0^\infty dq \int_{-1}^1 dt \left[\frac{q^2 E_k^{(-)} E_q^{(+)} + q^2 E_k^{(+)} E_q^{(-)}}{E_k + E_q + (k^2 - 2kqt + q^2)/\alpha} - \frac{2\alpha E_k^{(-)}}{\alpha + 1} \right] \\
\left. + \frac{k^2}{E_k + k^2/\alpha} \int_0^\infty dq q^2 \int_{-1}^1 dt \frac{\frac{k^2}{\alpha} + [\frac{2qt}{k} - 3] \left[E_k + E_q + \frac{q^2}{\alpha} \right]}{[E_k + E_q + (k^2 - 2kqt + q^2)/\alpha]^3} \left(E_k^{(-)} E_q^{(+)} + E_k^{(+)} E_q^{(-)} \right) \right\}. \quad (\text{S23})
\end{aligned}$$

Thus, the coefficients for the effective mass given by $\frac{m^*}{m} = 1 + F(\alpha)a^2/a_B\xi + G(\alpha)a^3/a_B\xi^2$ are

$$\begin{aligned}
F(\alpha) &= -\frac{\sqrt{2}}{3\pi} \frac{3(\alpha + 1) - 2(\alpha^2 + 2)f(\alpha)}{(\alpha + 1)(\alpha - 1)^2}, \\
G(\alpha) &= \frac{8}{3\pi^2} \frac{(1 + \alpha)^2(2 + \alpha^2) - 3(\alpha + 1)(3\alpha^2 + 1)f(\alpha) + 2\alpha^2(\alpha^2 + 5)[f(\alpha)]^2}{(\alpha - 1)(\alpha^2 - 1)^2} \\
&\quad - \frac{1}{2\pi^2} \left(\frac{\alpha + 1}{\alpha} \right)^3 \left(I_\omega(\alpha) + \frac{1}{3} I_{p^2}(\alpha) \right). \quad (\text{S24})
\end{aligned}$$

As stated in the main article the coefficients are well defined in the limit $\alpha \rightarrow 1$ and the values are stated in table I.

EXPANSION COEFFICIENTS FOR $\alpha = 0$, $\alpha = 1$ AND $\alpha = \infty$

	$A(\alpha)$	$B(\alpha)$	$C(\alpha)$	$D(\alpha)$	$F(\alpha)$	$G(\alpha)$
$\alpha \rightarrow 0$	$\frac{2\sqrt{2}}{\pi}$	1	∞	∞	∞	∞
$\alpha = 1$	$\frac{8\sqrt{2}}{3\pi}$	$\frac{2}{3} - \frac{\sqrt{3}}{\pi}$	$\frac{2\sqrt{2}}{3\pi}$	$\frac{64}{9\pi^2} - 0.080$	$\frac{16\sqrt{2}}{45\pi}$	$\frac{448}{135\pi^2} - 0.059$
$\alpha \rightarrow \infty$	$\sqrt{2}$	0	$\frac{1}{\sqrt{2}\pi}$	$\frac{2}{\pi} - 0.068$	0	0

TABLE I. Limiting values of the expansion coefficients for the energy, residue and effective mass.

CANCELLATION OF THE THIRD ORDER SELF-ENERGY INSERTION DIAGRAMS

To illustrate the cancellation of the third order diagrams obtained by self-energy insertions in the second order diagrams, we give here a specific example. Consider the third order diagram depicted in fig. S1, which is obtained by inserting a self-energy correction in the second order ladder diagram shown in Fig. 1(a). For zero momentum and temperature, this gives

$$n_0^2 \mathcal{T}_v^3 \int d\check{k} \frac{u_{\mathbf{k}}^2}{(\omega - E_{\mathbf{k}} - \epsilon_{\mathbf{k}})^2}. \quad (\text{S25})$$

When solving $E = \Sigma(E)$ for the impurity energy to third order in \mathcal{T}_v , it is enough to set $\omega = 0$ in Eq. (S25), whereas we have to insert the first order mean-field energy shift $\omega = n_0 \mathcal{T}_v$ in the second order diagrams. Inserting this energy shift in the diagram depicted in Fig. 1(a) and expanding yields

$$n_0 \mathcal{T}_v^2 \int d\check{k} \frac{u_{\mathbf{k}}^2}{n_0 \mathcal{T}_v - E_{\mathbf{k}} - \epsilon_{\mathbf{k}}} \simeq n_0 \mathcal{T}_v^2 \int d\check{k} \frac{u_{\mathbf{k}}^2}{-E_{\mathbf{k}} - \epsilon_{\mathbf{k}}} \left(1 + \frac{n_0 \mathcal{T}_v}{E_{\mathbf{k}} + \epsilon_{\mathbf{k}}} \right). \quad (\text{S26})$$

This explicitly demonstrates that the third order term in Eq. (S26) cancels the third order diagram given in Eq. (S25). Note that we have ignored the regularising term in the pair propagator in Eq. (S26), since it is irrelevant for the present purpose.

IMPURITY SELF-ENERGY FOR AN IDEAL BEC

For a non-interacting BEC, there is only one impurity Greens function, G_{11} , and we furthermore have $u_{\mathbf{k}} = 1$ and $v_{\mathbf{k}} = 0$ for the coherence factors. The pair propagator with $p = (\mathbf{p}, \omega)$ becomes the vacuum pair propagator given by [S44]

$$\Pi_{\text{vac}}(p) = -i \frac{m_r^{3/2}}{\sqrt{2\pi}} \sqrt{\omega - \mathbf{p}^2/2M}, \quad (\text{S27})$$

and the anomalous and particle-hole propagators both vanish. It follows that the second order self-energy is

$$\Sigma_2(p) = -in_0 \mathcal{T}_v^2 \frac{m_r^{3/2}}{\sqrt{2\pi}} \sqrt{\omega - \mathbf{p}^2/2M}. \quad (\text{S28})$$

The $\sqrt{\omega}$ dependence means that the residue vanishes for a zero momentum/energy impurity, and there is therefore no well-defined quasiparticle.

Furthermore, all third order diagrams vanish for $p = (\mathbf{0}, 0)$. The ladder diagrams depicted in fig. 2(a) are zero as they involve the vacuum pair propagator at zero energy/momentum, and/or the anomalous/particle-hole propagators. The crossed diagrams in fig. 2(c) are also all zero: Either they contain an integral over the particle-hole or the anomalous propagator which are both zero, or they contain the pair propagator multiplied by a hole propagator, which is zero for a non-interacting BEC. So all 2nd and 3rd order terms vanish for $p = (\mathbf{0}, 0)$ for a non-interacting BEC, meaning that mean-field theory is exact to third order for the energy of a $p = (\mathbf{0}, 0)$ impurity.